Bending loss and thermo-optic effect of a hybrid PDMS/silica photonic crystal fiber

Christos Markos,[1,2,*] Kyriakos Vlachos,[2] and George Kakarantzas[1]

[1]*National Hellenic Research Foundation, Theoretical and Physical Chemistry Institute, Athens, 11635, Greece*
[2]*Department of Computer Engineering and Informatics, University of Patras, Patra, 26500, Greece*
**cmarkos@eie.gr*

Abstract: In this paper, we demonstrate and report a photonic crystal fiber (PCF) infiltrated with PDMS elastomer which is sensitive to external bending and temperature perturbations. Numerical simulations and experimental measurements were carried out to investigate the fundamental TIR-based guiding mechanism of the hybrid PDMS/silica PCF in terms of effective index, effective modal area and loss. Wavelength dependence of bending losses was also measured for different bend diameters as well as the temperature dependence of the fundamental guiding mode for a range of temperatures from 20°C to 75°C. Experimental measurements have shown a ~6% power recovery of the bend-induced loss for a 6-cm long PDMS-filled PCF at 4 cm bend diameter.

OCIS codes: (060.5295) Photonic crystal fibers; (230.1150) All-optical devices; (160.2290) Fiber materials; (160.5470) Polymers; (060.2400) Fiber properties.

References and links

1. J. C. Knight, T. A. Birks, P. St. J. Russell, and D. M. Atkin, "All-silica single-mode optical fiber with photonic crystal cladding," Opt. Lett. **21**(19), 1547–1549 (1996).
2. A. Cerqueira S, Jr., F. Luan, C. M. B. Cordeiro, A. K. George, and J. C. Knight, "Hybrid photonic crystal fiber," Opt. Express **14**(2), 926–931 (2006).
3. L. Xiao, W. Jin, and M. S. Demokan, "Photonic crystal fibers confining light by both index-guiding and bandgap-guiding: hybrid PCFs," Opt. Express **15**(24), 15637–15647 (2007).
4. T. Larsen, J. Broeng, D. Hermann, and A. Bjarklev, "Thermo-optic switching in liquid crystal infiltrated photonic bandgap fibres," Electron. Lett. **39**(24), 1719–1720 (2003).
5. R. Bise, R. S. Windeler, K. S. Kranz, C. Kerbage, and B. J. Eggleton, "Tunable photonic band gap fiber," in Optical Fiber Communications Conference, A. Sawchuk, ed., Vol. 70 of OSA Trends in Optics and Photonics (Optical Society of America, 2002), paper ThK3.
6. C. M. Cordeiro, M. A. Franco, G. Chesini, E. C. Barretto, R. Lwin, C. H. Brito Cruz, and M. C. Large, "Microstructured-core optical fibre for evanescent sensing applications," Opt. Express **14**(26), 13056–13066 (2006).
7. S. Torres-Peiró, A. Díez, J. L. Cruz, and M. V. Andrés, "Fundamental-mode cutoff in liquid-filled Y-shaped microstructured fibers with Ge-doped core," Opt. Lett. **33**(22), 2578–2580 (2008).
8. C. G. Poulton, M. A. Schmidt, G. J. Pearce, G. Kakarantzas, and P. St. J. Russell, "Numerical study of guided modes in arrays of metallic nanowires," Opt. Lett. **32**(12), 1647–1649 (2007).
9. B. T. Kuhlmey, B. J. Eggleton, and D. K. C. Wu, "Fluid-Filled Solid-Core Photonic Bandgap Fibers," J. Lightwave Technol. **27**(11), 1617–1630 (2009).
10. P. S. Westbrook, B. J. Eggleton, R. S. Windeler, A. Hale, T. A. Strasser, and G. L. Burdge, "Cladding-Mode Resonances in Hybrid Polymer-Silica Microstrucutred Optical Fiber Gratings," IEEE Photon. Technol. Lett. **12**(5), 495–497 (2000).
11. Y. Fainman, L. P. Lee, D. Psaltis, and C. Yang, *Optofluidics: Fundamentals, Devices, and Applications* (McGraw-Hill, 2010)
12. J. C. Lötters, W. Olthuis, P. H. Veltink, and P. Bergveld, "The mechanical properties of the rubber elastic polymer polydimethylsiloxane for sensor applications," J. Micromech. Microeng. **7**(3), 145–147 (1997).
13. http://www.lumerical.com/fdtd.php
14. N. H. Vu, I.-K. Hwang, and Y.-H. Lee, "Bending loss analyses of photonic crystal fibers based on the finite-difference time-domain method," Opt. Lett. **33**(2), 119–121 (2008).
15. F. Schneider, J. Draheim, R. Kamberger, and U. Wallrabe, "Process and material properties of polydimethylsiloxane (PDMS) for Optical MEMS," Sens. Actuators A Phys. **151**(2), 95–99 (2009).

#134814 - $15.00 USD Received 17 Sep 2010; revised 27 Oct 2010; accepted 27 Oct 2010; published 5 Nov 2010

16. T. A. Birks, J. C. Knight, and P. St. J. Russell, "Endlessly single-mode photonic crystal fiber," Opt. Lett. **22**(13), 961–963 (1997).
17. J. C. Baggett, T. M. Monro, K. Furusawa, V. Finazzi, and D. J. Richardson, "Understanding bending losses in holey optical fibers," Opt. Commun. **227**(4-6), 317–335 (2003).
18. J. Olszewski, M. Szpulak, and W. Urbańczyk, "Effect of coupling between fundamental and cladding modes on bending losses in photonic crystal fibers," Opt. Express **13**(16), 6015–6022 (2005).
19. T. Martynkien, J. Olszewski, M. Szpulak, G. Golojuch, W. Urbanczyk, T. Nasilowski, F. Berghmans, and H. Thienpont, "Experimental investigations of bending loss oscillations in large mode area photonic crystal fibers," Opt. Express **15**(21), 13547–13556 (2007).
20. W. F. Yeung, and A. R. Johnston, "Effect of temperature on optical fiber transmission," Appl. Opt. **17**(23), 3703–3705 (1978).
21. H. R. Sørensen, J. Canning, J. Lægsgaard, and K. Hansen, "Control of the wavelength dependent thermo-optic coefficients in structured fibres," Opt. Express **14**(14), 6428–6433 (2006).

1. Introduction

Photonic crystal fibers (PCFs) are a class of optical fibers constituting a periodic array of air holes running along its length [1]. Infiltration of advanced materials into the air holes of the PCFs can potentially manipulate their optical properties creating a new category of fibers termed as hybrid PCFs [2,3]. Many hybrid devices such as switches [4], tunable devices [5], sensors [6,7] have been developed and studied by filling liquid crystal, high index fluids, metals [8] as well as other materials into the air holes by transforming an index guiding PCF into a photonic bandgap fiber (PBG) [9]. However, limited research has been so far carried out on the infiltration of PCF's holes with polymeric inclusions, conserving total internal reflection (TIR) guiding mechanism [10]. PDMS (poly-dimethylsiloxane) elastomer is a polymeric silicone material widely used in the area of photonics, particularly in opto/microfluidics, having unique optical properties [11]. Transparency for a wide range of wavelength, lower refractive index (around 1.41) than fused silica, high elasto-optic and thermo-optic coefficients, biocompatibility, minimal loss due to absorption, are some of its features. It also exhibits very good mechanical properties due to low Young's modulus; it is soft and deformable with no shrinkage and combined with its low cost, and ease fabrication procedure is a potential active material for tunable devices and sensing applications [12].

In this paper, we demonstrate for the first time to our knowledge the combination of the aforementioned polymeric material with PCF. We have investigated the basic guiding properties of the hybrid PDMS/silica PCF using Finite Time Difference Domain (FDTD) method and measure the total transmission loss at different wavelengths. Bend-induced loss properties of the hybrid PCF are experimentally demonstrated at 633 nm where the absorption loss of the elastomer material is very low, and 1550 nm wavelength in order to investigate the optical properties of the hybrid PDMS/silica PCF at infrared range. Bend measurements at 473 nm are also presented, emphasizing the sensitivity and short-wavelength bend loss edge of the fiber. Long-wavelength bend characteristics of the PDMS/silica PCF were measured at five different bend diameters utilizing a tunable laser source. Further numerical simulations made in order to investigate the temperature dependance of the PDMS-filled PCF under constant bending diameter of 4 cm. The negatively high linear thermo-optic coefficient of the elastomeric inclusions can partially reconstruct the fundamental guiding mode. Experimental measurements of a bent PDMS/silica PCF exhibited partial recovery of the transmitted power for a range of temperatures up to 75°C.

2. Experimental

In our experiments, we employed an ESM-PCF (ESM-12-02, Crystal Fibre) with a core diameter of 12 μm in which the air holes with diameter 3.5 μm are arranged in a hexagonal pattern with a pitch of 7.7 μm, as shown in Fig. 1(a). PDMS (Sylgard 184-Dow Corning) was prepared by mixing elastomer and curing agent at 10:1 ratio. A simple custom-build pressure cell was used to inject the material into the air holes of PCF. Figure 1(b) shows the scanning electron microscopy (SEM) image of the PDMS/silica PCF while (c) and (d) show the side view optical images of the conventional and the PDMS-infiltrated PCF, respectively. The fully filled part of the PCF had a length of about 6 cm.

#134814 - $15.00 USD Received 17 Sep 2010; revised 27 Oct 2010; accepted 27 Oct 2010; published 5 Nov 2010

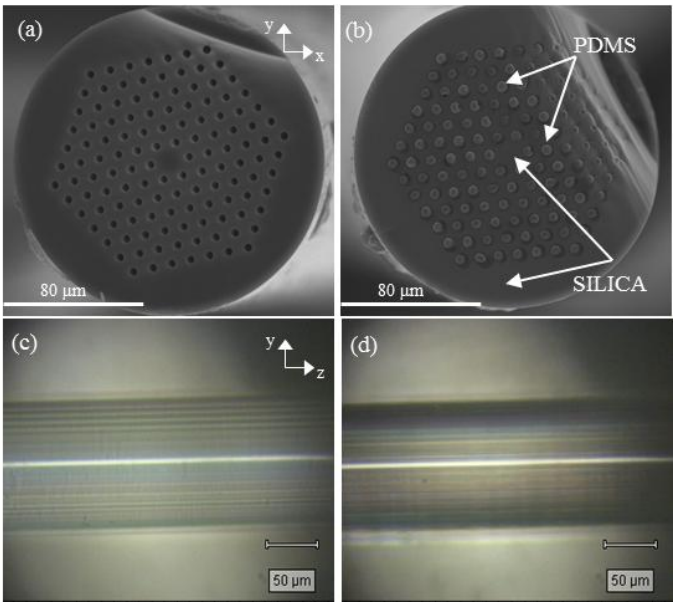

Fig. 1. Scanning-electron microscope (SEM) image of: (a) a conventional ESM-PCF supplied from Crystal Fibre (b) hybrid PDMS/silica PCF. Side view optical micrographs of (c) all-silica PCF and (d) PDMS-filled PCF.

3. Results and discussion

3.1 Guiding properties of PDMS/silica PCF

Numerical simulations based on FDTD analysis were performed using the commercial software package *Lumerical FDTD Solutions* [13,14] in order to investigate the guiding mechanism of the hybrid PDMS/silica structure. PDMS-filling fraction corresponded to 18.73%, where the low refractive index difference between silica and elastomer reduces the confinement of the fundamental guiding mode. Figures 2(a) and 2(b) illustrate the simulated mode profiles of the hybrid PDMS/silica PCF at 633 and 1550 nm, respectively. The effective modal areas were calculated to be $A_{eff} \approx 81.75 \mu m^2$ and 126.98 μm^2, at the aforementioned wavelengths, while for a conventional ESM-PCF these are $A_{eff} \approx 70.08 \mu m^2$ and $74.68 \mu m^2$, respectively.

Figure 2(c) shows the experimental near-field intensity pattern of the fundamental mode at 633 nm wavelength captured using a CCD camera. The calculated effective indices of the fundamental guiding mode of the conventional and PDMS/silica PCF are shown in Fig. 2(d) for a broad range of wavelengths. Real and imaginary parts of the refractive index of PDMS (Sylgard 184) - were calculated using the Sellmeier equation, where the coefficients have been experimentally determined in [15]. Total transmission loss of PDMS/silica fiber was measured using cut-back method and found to be equal to *~0.06 dB/cm* at 633 nm wavelength. The corresponding absorption coefficient of the material at this wavelength is very small [15]. At 1550 nm, transmission loss was increased to *~0.17 dB/cm*, since the confinement of the fundamental core mode was reduced, as compared to short wavelengths and the absorption coefficient of the material at infrared (IR) wavelengths is higher.

#134814 - $15.00 USD Received 17 Sep 2010; revised 27 Oct 2010; accepted 27 Oct 2010; published 5 Nov 2010

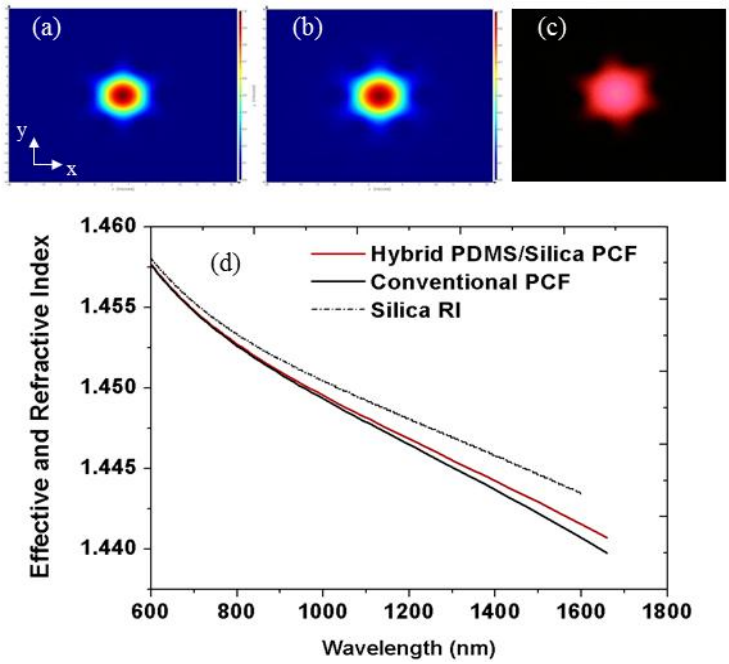

Fig. 2. (a) Calculated fundamental mode profile of the hybrid PDMS/silica PCF at 633 and (b) 1550 nm wavelength. (c) Experimental near field fundamental mode field pattern at 633 nm wavelength, captured with a CCD camera. (d) Effective indices of the fundamental guiding mode of a conventional (black line) and hybrid PDMS/silica PCF (red line). (Refractive index of fused silica is also included into the plot for reference purposes).

3.2 Bending loss properties

Bending loss of the hybrid PDMS/silica PCF was measured and compared with those of a similar all-silica PCF. We measured the output power for various bend diameters, *d*, applied in a circular loop with a single-turn of fiber and arbitrary angular orientation. Figures 3(a)–3(c) show the experimental measurements of the two fibers (conventional ESM and hybrid PDMS/silica PCF) at different wavelengths. The high bending sensitivity of PDMS/silica PCF, compared to the conventional PCF, can be clearly seen, particularly at short wavelengths. Short-wavelength bend loss edge of PCFs has been previously described using a simple effective index method [16]. The condition which defines the critical bend diameter can be written as:

$$d_C = \frac{16\pi^2 n_C^2 \rho^3}{\lambda^2 W^3} \tag{1}$$

In Eq. (1), n_c is the refractive index of the core, ρ is the core radius, while *W* is the modal parameter that is directly linked to cladding-core refractive index difference, *Δn*, of the fiber. In the case of the PDMS/silica PCF, *Δn* is smaller as compared to conventional PCFs and therefore exhibits a significantly higher sensitivity to bends. A fully detailed analysis on bending loss properties of photonic crystal fibers has been previously made in [17].

Figure 3(a) shows and compares bending losses for the two fibers (PDMS/silica and conventional PCF) at 463 nm wavelength. The dramatic increase of loss for bending diameters less than ~15 cm can be clearly seen. Figures 3(b) show the respective bending losses at 633 nm. In case of 1550 nm, the conventional ESM-PCF exhibits high loss at bend diameters less than 1.5 cm where the possibility of the fiber to break is high. In case of hybrid PCF, there is a three-fold increase in critical bend diameter due to PDMS inclusions, as can be seen from Fig. 3(c). It must be also noted here that the small localized peaks of the bending

#134814 - $15.00 USD Received 17 Sep 2010; revised 27 Oct 2010; accepted 27 Oct 2010; published 5 Nov 2010

losses appearing in our experimental results for both fibers - conventional and hybrid - are usually linked to the coupling between core and cladding "leaky" modes. This oscillatory character of losses versus bending diameter has been extensively investigated in [18,19].

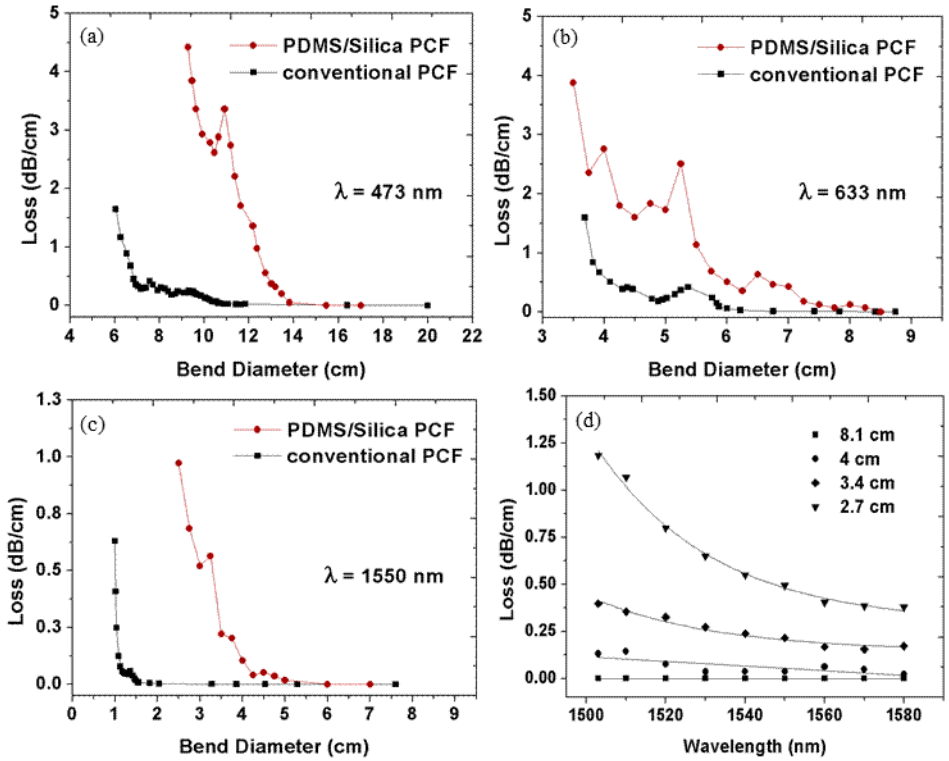

Fig. 3. Bending loss as a function of bend diameter at (a) 473, (b) 633 and (c) 1550 nm wavelength for a conventional and PDMS/silica PCF. (d) Measurement of bend loss variation as a function of wavelength for the case of hybrid PDMS/silica PCF at different bend diameters.

The wavelength dependence of the bending properties was also examined using a tunable C-band laser source at four different bending diameters. Figure 3(d) shows strong wavelength dependence for small bending diameters and short wavelengths and a relative weak (almost flat) dependence for large bending diameters and wavelengths ranged higher than 8.1 cm and 1570 nm, respectively. It is worth noting here, that the conventional ESM-PCF exhibited negligible bend loss for such bend diameters.

3.3 Thermo-optic effect

Normally, the temperature dependence of the refractive index is described by the thermo-optic coefficient d*n*/d*T*, which quantifies the shift of the refractive index arising from an infinitesimal change of the temperature. The PDMS elastomer, among the others optical properties mentioned previously, also exhibits a highly linear, negative thermo-optic coefficient corresponding to $dn/dT = -4.5x10^{-4}/\,°C$ [20]. Based on this change of refractive index with temperature, we calculated the corresponding effective indices of the fundamental guiding mode of the hybrid PDMS/silica PCF for different temperatures. Figure 4(a) and 4(b) show the effective index difference (Δn_{eff}) of each effective index calculated from 25 - 75°C, from the initial one calculated at room temperature (20°C) for the wavelengths of 633 and 1550 nm, respectively.. Δn_{eff} is almost an order of magnitude higher at 1550 nm, due to the low mode confinement and the large overlap between the guiding mode and cladding.

#134814 - $15.00 USD Received 17 Sep 2010; revised 27 Oct 2010; accepted 27 Oct 2010; published 5 Nov 2010

Figure 4(c) shows the effective modal area of the hybrid PCF for the same range of temperatures at 633 and 1550 nm.

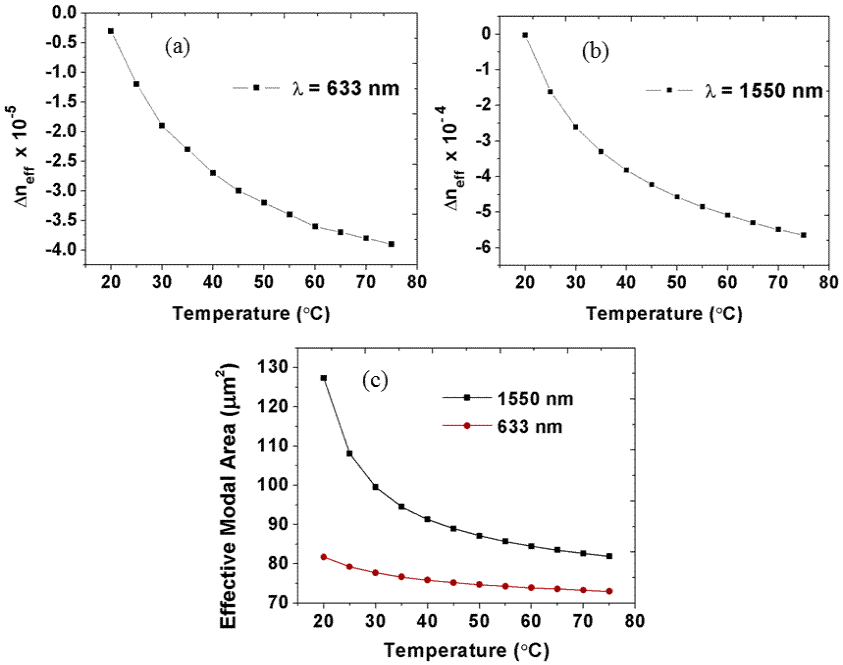

Fig. 4. Index difference variation, Δn_{eff} of PDMS/silica PCF as a function of temperature at (a) 633 nm and (b) 1550 nm operating wavelength. (c) Effective modal areas at 633 and 1550 nm wavelength.

Increasing the temperature, the refractive index contrast between cladding and core also increases, allowing for the fundamental guiding mode to be partially reconstructed back to the core of the fiber. FDTD analysis was performed for a temperature range of 20°C -to- 75°C and for a bend diameter of 4 cm. In Fig. 5, we present the electric field distribution (logarithmic scale) of the fundamental mode for a set of frames per 10°C from the simulation videos at 633 nm (see a - f) and 1550 nm (see g - l). In both cases the mode of the bent fiber is asymmetric in shape and shifts towards the outside of the bend near room temperature. As the temperature increases, the guiding mode starts accumulating at the core. At 633 nm the thermo-optic effect cannot overcome the high bend loss and the partial recovery of the fundamental mode is limited compared to 1550 nm.

#134814 - $15.00 USD Received 17 Sep 2010; revised 27 Oct 2010; accepted 27 Oct 2010; published 5 Nov 2010

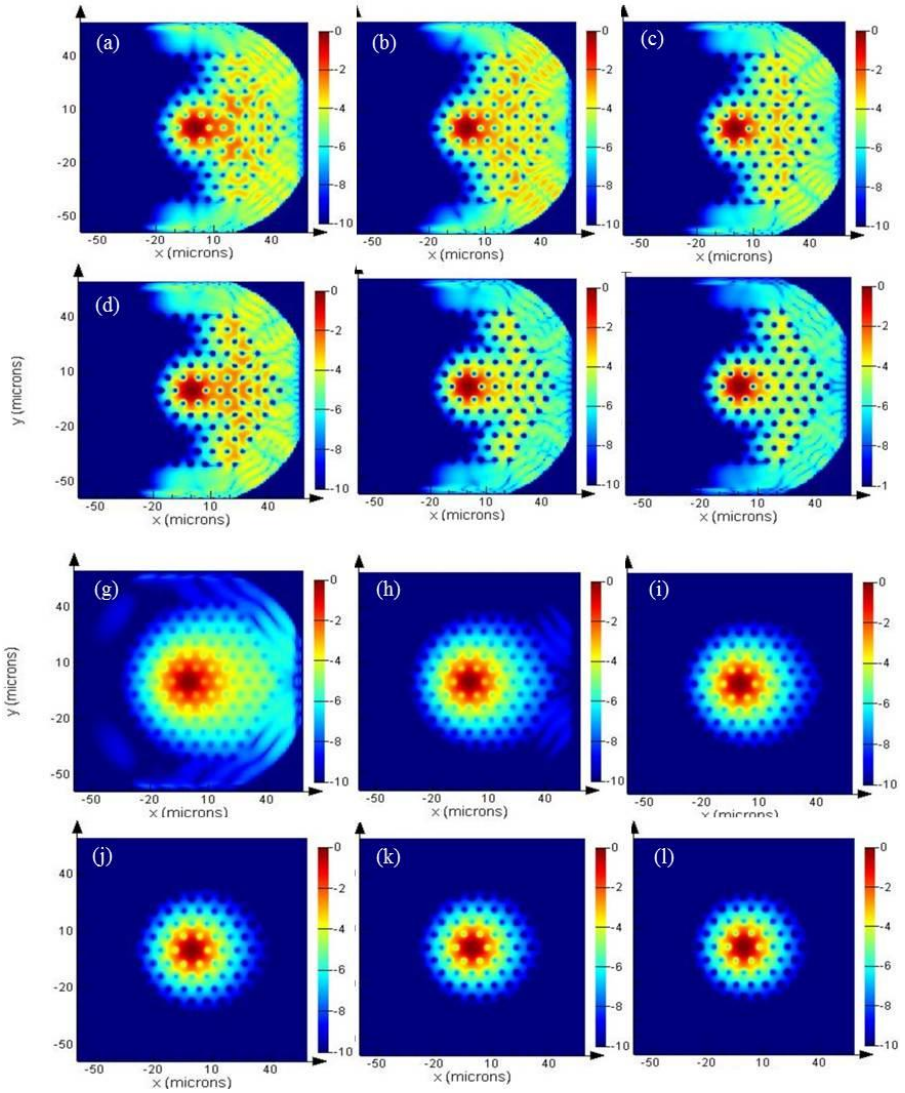

Fig. 5. Single-frame(one per 10°C) excerpts from two separate simulation videos illustrating the partial reconstruction of the fundamental guiding mode of the hybrid PDMS/silica PCF as temperature increases from 20°C to 75°C for a bend diameter of 4 cm. Frames (a-f) correspond to 633 (Media 1) and (g-l) to 1550 nm wavelength (Media 2) (logarithmic scale).

The thermo-optic sensitivity of the hybrid PCF, induced by the elastomer inclusion, was also investigated experimentally. We placed the hybrid PCF at a bend diameter of 4 cm on top of a peltier element with perfect thermal contact to the surface. Using a laser source, a power meter, and a thermo-couple we measured the amount of power recovered from the bending induced loss. Figure 6(a) shows how bending loss varies with the increase of temperature at 633 nm and clearly shows a recovery of ~3.6% of the total transmitted power, at 75°C. Same measurements were repeated at 1550nm, investigating the thermo-optic sensitivity at longer wavelengths and the bend-induced power loss recovery corresponded to 5.93%. Results are shown in Fig. 6(b). Slight discrepancies appeared in our experimental results derived from a combination of losses arising in the fabrication process and experimental characterization of the device (absorption due to impurities, scattering, human error, etc.). The temperature sensitivity was defined as ΔPower/ΔTemp and estimated to be 0.05 dB/°C at 633 nm and 0.005 dB/°C at 1550 nm. In the case of the conventional ESM-PCF, power was unrecoverable

#134814 - $15.00 USD Received 17 Sep 2010; revised 27 Oct 2010; accepted 27 Oct 2010; published 5 Nov 2010

either at 633nm or 1550 nm wavelength due to very small thermo-optic coefficient of fused silica [21].

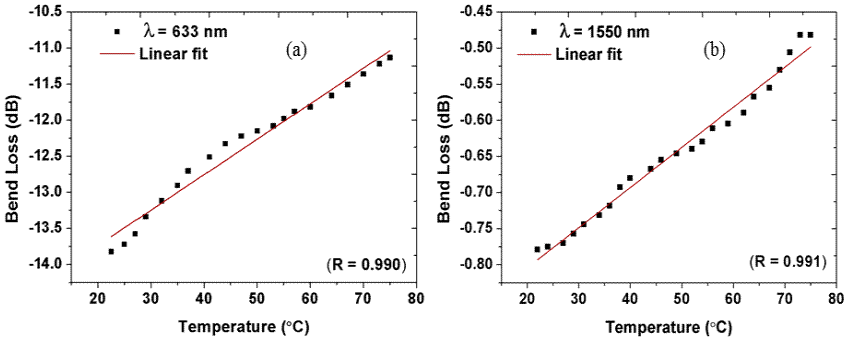

Fig. 6. Thermo-optic effect of PDMS-filled PCF for a bend diameter of 4 cm at (a) 633 and (b) 1550 nm.

4. Conclusion

In conclusion, we have demonstrated for the first time towards our knowledge, a hybrid PDMS/silica PCF. We examined the guiding mechanism of the hybrid fiber, where acceptable level of loss measured over short lengths. Bend measurements of the PDMS/silica PCF at different wavelengths were carried out, demonstrating the dramatic shift of the short and long bend loss edge to higher bend diameters compared to a conventional PCF. Further numerical calculations indicated the dependence of the effective index of the fundamental guiding mode of PDMS/silica PCF with temperature and we demonstrated how the fundamental mode of a bent fiber can be reconstructed due to thermo-optic effect of the PDMS inclusions. It was also experimentally shown that there was a ~6% bend-induced power loss recovery at a range of temperatures up to 75°C. The hybrid PDMS/silica PCF has the potential to be used for macro-bend sensing, whereas the feature of power recovery with temperature, further enhances the ability of the fiber to act as temperature-tuned device over a wide range of wavelengths. Finally, it is relatively simple to be developed using commercially available PCFs and a low cost elastomer material.

Acknowledgments

The authors acknowledge financial support from the project SESAMO of the European Defence Agency (EDA) with Grant No. A-0931-RT-GC.

#134814 - $15.00 USD Received 17 Sep 2010; revised 27 Oct 2010; accepted 27 Oct 2010; published 5 Nov 2010